DEPARTMENT OF PHYSICS, UNIVERSITY OF JYVÄSKYLÄ
RESEARCH REPORT No. 7/1999

MAGNETIC PROPERTIES OF SMALL CLUSTERS OF SPINS

BY
EERIK VIITALA

Academic Dissertation
for the Degree of
Doctor of Philosophy

Jyväskylä, Finland
December 1999

URN:ISBN:978-951-39-9752-6
ISBN 978-951-39-9752-6 (PDF)
ISSN 0075-465X

Jyväskylän yliopisto, 2023

ISBN 951-39-0622-1
ISSN 0075-465X

DEPARTMENT OF PHYSICS, UNIVERSITY OF JYVÄSKYLÄ
RESEARCH REPORT No. 7/1999

MAGNETIC PROPERTIES OF SMALL CLUSTERS OF SPINS

BY
EERIK VIITALA

Academic Dissertation
for the Degree of
Doctor of Philosophy

To be presented, by permission of the
Faculty of Mathematics and Natural Sciences
of the University of Jyväskylä,
for public examination in Auditorium FYS 1 of the
University of Jyväskylä on December 17, 1999,
at 12 o'clock noon

Jyväskylä, Finland
December 1999

Preface

The studies reviewed in this thesis have been carried out during the years 1994-1999 in the Department of Physics at the University of Jyväskylä. First of all I wish to express my sincere gratitude to my supervisors, Prof. Jussi Timonen and Prof. Matti Manninen for excellent guidance I received throughout the work. I am also deeply indebted to Dr. Juha Merikoski, Dr. Hannu Häkkinen and Dr. John Parkinson for the pleasant and fruitful collaboration. I would also thank the other members of JYFL staff for providing an excellent working atmosphere.

The financial support from the Yrjö, Vilho and Kalle Väisälä Foundation, the University of Jyväskylä and the Academy of Finland are gratefully acknowledged.

Last but not the least I want to thank from all my heart my wife Sari and my daughters Iida and Anna-Maija for the wonderful moments they have given to me.

Jyväskylä, December 1999

Eerik Viitala

Abstract

This thesis reviews three publications and also describes some further results that have not yet been published. In these works three different topics concerning the magnetic properties of small atomic clusters have been considered: the magnetic behaviour of antiferromagnetic Ising clusters, the possibility to use effective spin Hamiltonians to describe the magnetic properties of small nickel clusters, and the nature of zero-temperature phase transitions of small antiferromagnetic Heisenberg clusters in the classical limit.

The Ising model is used to numerically investigate the magnetic properties of small antiferromagnetic clusters with nearest-neighbour interactions. The possibility is investigated to use a superparamagnetic model, an interesting form of magnetism found for ferromagnetic Ising and Heisenberg clusters, also for the antiferromagnetic Ising clusters. The influence of the underlying lattice structure on the magnetic properties is demonstrated. Also, the effects due to incomplete atomic shells in the clusters, and to randomness of the coupling constants, are considered. All numerical computations have been done exactly, which caused us to restrict the considered size of the clusters to 30 atoms or less.

Spin Hamiltonians have been used to describe the magnetic behaviour of bulk matter for more than half a century, and many significant results related to these problems have been obtained. However, surprisingly little is known about the effective spin Hamiltonians appropriate for small atomic clusters. In this work the possibility to use effective spin Hamiltonians for small nickel clusters to explain their magnetic properties is considered. Questions concerning the terms that should be included in these spin Hamiltonians, and the lengths of single spins of the models, have been posed, and some answers to these questions could be given. It turned out that the appropriate spin Hamiltonian is strongly dependent on the number of spins and the structure of the atomic clusters.

In the classical limit of the Heisenberg model with antiferromagnetic exchange interaction, a phenomenon analogous to zero-temperature phase transitions can be observed in certain clusters. Group theoretical methods were used to analyse the properties of these transitions. For the first time the magnetic symmetry of a classical spin system was obtained. We also suggest how to define the symmetry in the classical case and provide numerical evidence for it. Also, a sufficient condition for a zero-temperature phase transition to occur in the classical limit is conjectured.

List of publications

This thesis reviews the following publications:

I Properties of small antiferromagnetic Ising clusters
E. Viitala, J. Merikoski, M. Manninen and J. Timonen
Z. Phys. D **40**, 173 (1997).
https://doi.org/10.1007/s004600050187

II Antiferromagnetic order and frustration in small clusters
E. Viitala, J. Merikoski, M. Manninen and J. Timonen
Phys. Rev. B **55**, 11541 (1997).
https://doi.org/10.1103/PhysRev B.55.11541

III Spin Hamiltonians for small Ni clusters
E. Viitala, H. Häkkinen, M. Manninen and J. Timonen
Phys. Rev. B, in press.
https://doi.org/10.1103/PhysRev B.61.8851

IV Quantum to classical transition for small magnetic cluster in an external magnetic field
J. B. Parkinson, R. J. Elliot, E. Viitala and J. Timonen
To be published.
https://doi.org/10.1088/0953-8984/14/1/305

The author of this Thesis has actively taken part in writing papers I and II and has done all numerical analysis related to the effects of incomplete shells, locally modified coupling strengths and finite size. Paper III is written by the author and he has done all the numerical computations. For the forthcoming IV the author has done numerical work related to the computation of symmetries of spin configurations and contributed actively to the interpretation of the results.

Contents

1 Introduction

Well controlled experiments on magnetic properties of small transition metal clusters (Fe and Co) became possible in the early 90's[1, 2, 3, 4]. The experimental setup used was that of the Stern-Gerlach experiment[5] with accurate mass control of the clusters. When a magnetic cluster enters an inhomogeneous magnetic field, it is deflected into the direction of increasing field. By measuring the deflection profile as a function of external parameters, the temperature of the clusters and the value of the external field, it was possible to extract information about the cluster magnetism. The results for small ferromagnetic clusters cited above were then interpreted within the superparamagnetic model[6, 7], an interesting model of magnetism in which the cluster behaves as a large paramagnetic spin.

These earliest studies concentrated on the properties of ferromagnetic clusters. Later on theoretical interest turned to the properties of small antiferromagnetic clusters[9, I, II]. Reddy and Khanna in Ref. [9] used the Monte Carlo method and concentrated on clusters with complete shells in low external fields and at low temperatures. In Refs. I and II this picture was sharpened by a detailed study of magnetic ordering in different geometries and lattice structures. Also, the magnetic properties of clusters with incomplete shells were considered together with the effect of variations in the coupling constants.

Spin models have been used for a long time to study bulk magnetism[8] but very little is known about the possibility to use spin models to describe magnetism of small clusters. To investigate how well the spin Hamiltonian formalism can describe the magnetic behaviour of small clusters, one needs to know the energies and the magnetic moments of the lowest lying excited states. Unfortunately these kind of data are not known at present. Therefore we did 'computer experiments' and used numerical simulations to obtain the lowest lying electronic states and their magnetic moments. In Ref. III we used density functional theory to compute the electronic structure of small nickel clusters. We investigated the effects of size and symmetry of the cluster on the form of the effective spin Hamiltonian, and on the values of the spin Hamiltonian parameters.

At zero temperature the magnetisation of the antiferromagnetic Heisenberg model with finite spin length shows a step structure as a function of external field. This is caused by level crossings as the ground state changes when the external field increases. Parkinson and Timonen showed by numerical simulations that only a few if any of these steps survive in the classical limit[10] in the form of cusps in the zero-temperature magnetisation curve. In Ref. IV we will use group theoretical methods to obtain the conditions under which a transition found in the zero-temperature quantum system remains such also in the classical limit.

Theory

2 Computation of electronic structure

The quantum mechanical treatment of a many-body system is a very difficult problem. In fact as simple a system as a helium atom with two electrons lacks exact solution although we can solve this problem very accurately using approximative methods. During the last decades numerous highly sophisticated approximations to solve many-body Schrödinger equations have been developed. In many cases the state space is confined in some way, i.e. the allowed form of the wave function is restricted as e.g. in Hartree-Fock theory, in which the allowed wave functions are of determinant form.

2.1 Density Functional Theory

One of the most accurate methods for calculating the energy levels of many-body systems is the density functional theory (DFT) developed by Hohenberg, Kohn and Sham in the middle of the 1960's[11, 12]. In that theory the basic variable is electron density $\rho(\mathbf{r})$ instead of wave function. Thus the complicated wave function of $3N$ variables is replaced by a function of only three variables. This results in a considerable simplification.

The first model, which can be treated as a special case of the current form of DFT, was the Thomas-Fermi model developed in the late 1920's. In this model one can already find one of the main ideas of DFT: the so-called local density approximation. In this case it means that the kinetic energy of the nonhomogeneous electron density can be calculated as a sum (integral) of local kinetic energies defined by the homogeneous electron density.

2.1.1 Theoretical basis of DFT

Logically DFT can be divided into two parts. The first part consists of the Hohenberg-Kohn theorems[11], which give a theoretical justification for the use of the electron density as the basic variable instead of the wave function. These theorems also determine the correct electron density which is realised in nature out of the infinite number of available possibilities. The second part provides a practical method to find the correct electron density related to the physical system of interest. This procedure was developed by W. Kohn and L. Sham [12], and the result is the famous Kohn-Sham equations.

Theorem 1. The external potential of a system $v(\mathbf{r})$ is determined, within a constant, by the ground state electron density $\rho(\mathbf{r})$ of the system.

This theorem shows that the electron density ρ of the system determines its external potential

v, and, in addition, the number of electrons N in a natural way, $N = \int \rho(\mathbf{r})d\mathbf{r}$. Thus the Schrödinger equation of the system and its solutions are determined by the electron density. Therefore, at least in principle, the electron density defines all properties of the system, and we can write the expectation value of any operator as a functional of the electron density. The total energy of the system can then be written as a sum of the kinetic energy $T[\rho]$, the interaction energy of the external potential $V_{ne}[\rho]$ and the electron-electron interaction energy $V_{ee}[\rho]$,

$$E_v[\rho] = T[\rho] + V_{ne}[\rho] + V_{ee}[\rho]\,. \tag{1}$$

The electron-electron repulsion term $V_{ee}[\rho]$ consists of two parts: the classical electrostatic energy

$$J[\rho] = \frac{1}{2}\int \frac{\rho(\mathbf{r})\rho(\mathbf{r}')}{|\mathbf{r}-\mathbf{r}'|}d\mathbf{r}d\mathbf{r}' \tag{2}$$

and the exchange-correlation energy, which contains the non-classical effects.

A proof of Theorem 1 as well as of Theorem 2 below, can be found for instance in Ref. [13].

Theorem 2. If E_0 is the ground state energy of a system, i.e. $E_0 = E_v[\rho_0]$, then for every other density ρ' such that $N = \int \rho'(\mathbf{r})d\mathbf{r}$ and $\rho'(\mathbf{r}) \geq 0$,

$$E_0 \leq E_v[\rho']\,. \tag{3}$$

Theorem 2 states that the correct electron density $\rho_0(\mathbf{r})$, which is realised in nature, is the one that gives the minimum value for the total energy. Thus, to find the electron density with the lowest energy, one needs to solve a variational problem with a constraint for the number of electrons,

$$\delta\left\{E_v[\rho] - \mu\left[\int \rho(\mathbf{r})d\mathbf{r} - N\right]\right\} = 0. \tag{4}$$

Given the ground state electron density ρ_0, there exists a large (in fact an infinite) number of antisymmetric wave functions that produce the same electron density ρ_0. However, using the minimum energy principle, it is possible to distinguish the correct ground state wave function Ψ_0 because for all the other wave functions Ψ that give the same density ρ_0, we have

$$\begin{aligned} \langle\Psi|H|\Psi\rangle &> \langle\Psi_0|H|\Psi_0\rangle \\ \langle\Psi|T+V_{ee}|\Psi\rangle + \int \rho_0(\mathbf{r})v(\mathbf{r})d\mathbf{r} &> \langle\Psi_0|T+V_{ee}|\Psi_0\rangle + \int \rho_0(\mathbf{r})v(\mathbf{r})d\mathbf{r} \\ \langle\Psi|T+V_{ee}|\Psi\rangle &> \langle\Psi_0|T+V_{ee}|\Psi_0\rangle\,. \end{aligned} \tag{5}$$

This shows that to obtain the correct wave function that gives the ground state electron density ρ_0, we must minimise the functional F defined by

$$F[\rho] = \langle\Psi|T+V_{ee}|\Psi\rangle\,. \tag{6}$$

2.1.2 Kohn-Sham equations

The above section provides a theorectical basis to use the electron density as a basic variable instead of the wave function. This is the message of the first theorem of Hohenberg and Kohn. The second theorem gives a criterion for how to find the correct electron density. It is the one that gives the lowest total energy. Now we turn to the question of how a correct function $\rho(\mathbf{r})$ can be determined in practice. The procedure is called the Kohn-Sham method and the correct electron density can be obtained by solving the Kohn-Sham equations.

Kohn and Sham showed that it is possible to reformulate the problem in terms of noninteracting electrons. In this new form the kinetic energy of the system can be handelled exactly. However, this leads to a supposedly small correction to the original kinetic energy, and therefore we must reformulate also the functional $F[\rho]$. If $\rho_0(\mathbf{r})$ is the ground state electron density, there exist a potential $v(\mathbf{r})$ and the related Schrödinger equation (in atomic units)

$$\left[-\frac{1}{2}\nabla^2\psi_i + v(\mathbf{r})\right]\psi_i = \epsilon_i\psi_i\,, \tag{7}$$

such that the ground state wave function of determinant form $\Psi = \det[\psi_1\psi_2\ldots\psi_N]$ exactly gives the electron density ρ_0. The kinetic energy T_s of this new system is

$$T_s[\rho] = \langle\Psi|\sum_{i=1}^{N} -\frac{1}{2}\nabla_i^2|\Psi\rangle = \sum_{i=1}^{N}\langle\psi_i| - \frac{1}{2}\nabla_i^2|\psi_i\rangle\,. \tag{8}$$

If T and T_s are the kinetic energies of the original and the new system, respectively, F can be written in the form

$$F[\rho] = T_s[\rho] + J[\rho] + E_{xc}[\rho]\,, \tag{9}$$

where

$$E_{xc}[\rho] = T[\rho] - T_s[\rho] + V_{ee}[\rho] - J[\rho] \tag{10}$$

is the exchange-correlation energy. Thus the total energy of the original system is

$$E[\rho] = \sum_{i=1}^{N}\sum_{s}\int\psi_i^*(\mathbf{r},s)(-\frac{1}{2}\nabla_i^2)\psi_i(\mathbf{r},s)d\mathbf{r} + J[\rho] + E_{xc}[\rho] + \int\rho(\mathbf{r})v(\mathbf{r})d\mathbf{r}\,. \tag{11}$$

According to the second theorem of Hohenberg and Kohn, the total energy functional $E[\rho]$ attains its minimum for the correct electron density. Instead of making a variational search directly through the electron density ρ, we can do the search in the orbital space $\{\psi_i\}$. However, the orbitals need to be orthonormal and one must solve a variational problem with constraints,

$$\delta\left\{E[\rho] - \epsilon_{ij}\left[\sum_{s}\sum_{i,j=1}^{N}\int\psi_i^*(\mathbf{r},s)\psi_j(\mathbf{r},s)d\mathbf{r} - \delta_{ij}\right]\right\} = 0 \tag{12}$$

where ϵ_{ij} are Lagrange undetermined multipliers. The solution of this variational problem leads to the famous Kohn-Sham equations

$$-\frac{1}{2}\nabla^2\psi_i \;+\; v_{eff}(\mathbf{r})\psi_i = \epsilon_i\psi_i \tag{13}$$

$$v_{eff}(\mathbf{r}) = v(\mathbf{r}) + \int \frac{\rho(\mathbf{r}')}{|\mathbf{r}-\mathbf{r}'|} d\mathbf{r}' + \frac{\delta E_{xc}[\rho]}{\delta \rho(\mathbf{r})} \tag{14}$$

$$\rho(\mathbf{r}) = \sum_{s} \sum_{i=1}^{N} |\psi_i(\mathbf{r}, s)|^2 , \tag{15}$$

where N is the number of electrons. The original problem has now been formulated in the independent-electron form. Although the explicit form of the exchange-correlation energy is not known, these equations are exact in principle, and have also several advantages which make them attractive to use. All the difficulties due to many-body interactions between electrons are hidden in the exchange-correlation energy E_{xc}. The simplest approximation for the exchange-correlation energy proposed by Kohn and Sham is called the local-density approximation (LDA). The idea is to use the uniform electron gas formula locally for the exchange-correlation energy. This leads to the approximation

$$E_{xc}^{LDA}[\rho] = \int \rho(\mathbf{r}) \epsilon_{xc}(\rho) d\mathbf{r} , \tag{16}$$

where ϵ_{xc} is the exchange-correlation energy per particle of a uniform electron gas of density ρ. To approximate ϵ_{xc} numerous proposals have been made.

For a spin-polarised system the basic variables are the electron densities $\rho^{\alpha}(\mathbf{r})$ and $\rho^{\beta}(\mathbf{r})$ for up and down spins, respectively, and the total electron density is $\rho(\mathbf{r}) = \rho^{\alpha}(\mathbf{r}) + \rho^{\beta}(\mathbf{r})$. In this form the theory is called spin-density-functional theory. Using the same kind of procedure as described above for the non-polarised case, it is possible to derive the Kohn-Sham equations for the spin-polarised system in the form

$$\left[-\frac{1}{2}\nabla^2 + v_{eff}^{\sigma}(\mathbf{r}) \right] \phi_{i\sigma}(\mathbf{r}) = \epsilon_{i\sigma} \phi_{i\sigma}(\mathbf{r}) \tag{17}$$

$$v_{eff}^{\sigma}(\mathbf{r}) = v(\mathbf{r}) + \int \frac{\rho(\mathbf{r}')\mathbf{d}\mathbf{r}'}{|\mathbf{r}-\mathbf{r}'|} + \frac{\delta \mathbf{E}_{\mathbf{xc}}[\rho^{\alpha}, \rho^{\beta}]}{\delta \rho^{\sigma}(\mathbf{r})} \tag{18}$$

$$\rho^{\sigma}(\mathbf{r}) = \sum_{i=1}^{N} |\phi_{i\sigma}(\mathbf{r})| , \tag{19}$$

where N is the number of electrons in the system, α and β denote up and down spins, respectively, and ρ^{σ} is the electron density for spin σ; $\sigma = \alpha, \beta$. In the spin-polarised case the LDA-approximation is replaced by the local-spin-density approximation (LSDA). Thus the exchange-correlation energy is approximated by a homogeneous spin-polarised electron gas instead of a homogeneous spin-compensated electron gas. Among the several advantages of the DFT-LSDA method is that it can be applied to systems with spontaneous magnetisation.

It should be evident from the discussion of the DFT formalism above that approximating the exchange-correlation energy is an essential ingredient in the Kohn-Sham equations. Thus its (approximative) form may have considerable influence on the solutions and the energy spectrum of the system. Considering the present work, it may have had some influence

on the results obtained in Ref. [III] for the possibility to use spin Hamiltonian formalism to describe the magnetism of small nikel clusters. A systematic investigation of the effects of different approximative forms of the exchange-correlation energy will be considered in forthcoming publications.

The form of DFT presented here (as also in the computations of the electronic structures in Ref. [III]) does not take into account the possible current densities in the system. Therefore, the effect of orbital angular momenta on the magnetism of small clusters is ignored. It is possible to include these effects into the formalism of DFT and use the so-called current- and spin-density-functional theory[14]. It remains to be seen if this will affects the results obtained in Ref. [III].

In addition to the methods described above, these are many other methods which have been used to determine the electronic structure of small atomic clusters and molecules. For instance the tight-binding method and the Hubbard model[15] have recently been used to obtain the electronic structures of clusters[38, 43]. However, these methods have same deficiency as the DFT-LSDA method used in Ref. [III], the magnetic moments related to the orbital angular momenta are lacking.

3 Spin models

In a purely classical theory magnetism does not exist[16], and, therefore, to explain the magnetic properties of a solid we need a quantum mechanical description of the material. This means that in order to obtain information related to the magnetic properties of a system, we have to solve its Schrödinger equation which in general is a very difficult task. As described briefly in Sec. 2, several kinds of models, which can be solved numerically, have been developed during the last few decades. The so-called *ab initio* methods, which do not have parameters to be fitted, are the best methods available at the moment, and can handle atomic clusters from ten to a couple of hundred of atoms depending on the number of electrons per atom involved in the computation. A spin model is an attempt to circumvent the difficulties which arise in solving the many-body Schrödinger equation when increasing the number of electrons. The spin model is a highly idealised model, which compresses a large amount of information related to the electronic structure of a system to a few parameters that can be fitted to give the correct energy and magnetic spectrum. In principle it is possible to calculate the values of the spin model parameters from the electronic structure of the system but, this is still an unsolved problem[17, 18].

There are two main questions related to the spin models. First of all one should know when it is possible to use a spin model, and secondly what kind of terms should be included in it. For both of these questions some results are known, but they can only be considered as sufficient conditions[8]. Futhermore, it is difficult to confirm whether the assumptions made to obtain these results are valid in practical situations. Also, the length of the spin to be

used in these spin models needs to be more carefully analysed in the context of small atomic clusters.

One thing should be made clear when spin models are used. The exchange interaction is not a real interaction between spins in the same sense as for instance the Coulomb interaction. The true interaction responsible for the magnetic properties is the Coulomb force. Therefore, effective spin Hamiltonians are phenomenological. They try to describe the magnetic properties of a system without making reference to its electronic degrees of freedom. But this is very common in physics, a model is useful when it can describe in a consistent way the observed properties of a system.

3.1 The sources of magnetism

Electrons are the main source of magnetism and therefore the magnetic properties of a system (from atoms to the bulk) are related to its electronic properties. There are two different sources of magnetism due to the electrons which are roughly equal. First the electrons have an intrinsic angular momentum, called the spin, which gives rise to a magnetic moment. Furthermore, the electrons have orbital angular momenta which also generate magnetic moments. There is a wide variety of possibilities how these properties evolve when more and more atoms are put together. This diversity strongly depends on the atomic electron configurations and the impurities of the system.

Only partially filled elecronic shells give a contribution to magnetism, except for a very small diamagnetic effect due to the contribution of filled shells. Diamagnetic susceptibility is of the order of $10^4 - 10^5$ times smaller than the susceptibility related to the partially filled shells.

3.2 Exchange interaction

A term related to the exchange interaction is the first term which is known to be included in an effective spin Hamiltonian. The concept of exchange was first introduced by Heitler and London when they explained chemical bonding[19]. Soon after this Dirac published his vector model for atoms[20]. Van Vleck[21] and Møller[22] generalised Dirac's concept, and they introduced the so-called effective spin Hamiltonian. Ever since the spin Hamiltonian formalism has been important in the field of magnetism.

The physical picture behind the exchange interaction is related to the behaviour of a wave function under the exchange of coordinate and spin indices. The antisymmetry principle causes the electrons with the same spin to avoid each other, and it therefore seems that the interaction strength between the electrons depends on their spin quantum numbers. This is nicely demonstrated for the hydrogen molecule in Ref. [16]. When atoms are near each other the wave functions of the outermost orbitals begin to overlap. Thus an electron

found initially around atom i may later be found around atom j. This process of exchange of two electrons between atoms i and j is described by the Heisenberg type Hamiltonian

$$\begin{aligned} \mathcal{H} &= \sum_{<i,j>} J_{ij} \mathbf{S}_i \cdot \mathbf{S}_j \\ &= \sum_{<i,j>} \frac{J_{ij}}{2} \left(S_i^+ S_j^- + S_i^- S_j^+ \right) + \sum_{<i,j>} J_{ij} S_i^z S_j^z \,, \end{aligned} \tag{20}$$

in which the combinations of the rising and lowering spin operators $S_j^{\pm} = S_j^x \pm i S_j^y$ are responsible for the exchange of two electrons. In Eq. 20 it is assumed that atoms i and j are still so far away from each others that only the exchange of one electron pair is likely to occur at a time. Otherwise higher order exchange terms should be present to allow for simultaneous exchange of two or more electron pairs between atoms i and j. Furthermore it is assumed that the distance between next-nearest neighbours is so large that exchange of an electron pair between them is highly improbable. Thus the sum in Eq. 20 is restricted to the nearest neighbours. The parameter J_{ij} is the exchange coupling constant and it describes the probability for the exchange to occur.

Taking into account an applied field B, an interaction term between the field and a spin must be added to the Eq. 20. Thus, with an applied field, the Heisenberg Hamiltonian reads

$$\mathcal{H} = \sum_{<i,j>} J_{ij} \mathbf{S}_i \cdot \mathbf{S}_j - B \sum_{i=1}^{N} S_i^z \,, \tag{21}$$

where N is the number of spins. It is assumed in Eq. 21 that the field B is applied in the direction of the z axis.

3.3 Crystal field and higher powers of components of spin operators

Treating the spin-orbit coupling $\lambda \mathbf{L} \cdot \mathbf{S}$ by second order perturbation theory shows that a second order term which operates in the spin space gives a contibution to the energy, and therefore second order terms must also be included in the effective spin Hamiltonian[24]. However, the generally used second order perturbation theory means that only terms up to second order with respect to the coupling strength λ are taken into account. Third and higher order terms with respect to λ should in principle also appear in the perturbation series, and hence also in the effective spin Hamiltonian. The crystal structure of a solid can produce additional direction dependent (an inhomogeneous electric field) terms for the local

magnetic moments through coupling of the orbital angular momenta of the electrons with this electric field. Depending on the symmetry of the system and the perturbations caused by the crystal environment, different kinds of effective spin Hamiltonians can be relevant. This can lead to a spin Hamiltonian of the form

$$H_{eff} = J \sum_{<i,j>} \mathbf{S}_i \cdot \mathbf{S}_j + A \sum_{i=1}^{N} (S_i^z)^2 + C \sum_{i=1}^{N} (S_i^z)^3 + D \sum_{i=1}^{N} (S_i^z)^4 \,, \tag{22}$$

used in this work. Notice that the exchange coupling constant is assumed to have the same value for all pairs of spins, i.e. $J_{ij} = J$. This is true for all small nickel clusters considered in Ref. [III] because all lattice sites of the clusters are equivalent. Also terms like $(S_i^+)^2 + (S_i^-)^2$ and $(S_i^+)^4 + (S_i^-)^4$ are possible[26, 27], but in this work these are neglected because the z component of the total spin must be a good quantum number.

Depending on the sign of the exchange coefficients J_{ij} in Eq. 21, the Heisenberg Hamiltonian favours parallel ($J_{ij} < 0$) or antiparallel ($J_{ij} > 0$) alignment of the nearest-neighbour spins. As mentioned above, the crystal environment can cause highly inhomogeneous electric fields which produce additional interactions that may tend to align the spins e.g. in a definite direction in space. If these interactions are strong enough, one may get a situation in which the spins are likely to point in one of the two possible directions along a particular axis. In this case the spin operators in Eq. 21 become scalar valiables. This situation is described by the Ising model[23] in which the magnetic energy E of a spin configuration $\{S_i\}$ is

$$E(\{S_i\}) = \sum_{<i,j>} J_{ij} S_i S_j - B \sum_{i=1}^{N} S_i \,, \tag{23}$$

where $S_i = \pm 1$ for all i.

3.4 About the classical limit of the AFM Heisenberg model

In a numerical investication of the AFM Heisenberg model Parkinson and Timonen found that cusps may appear at zero-temperature in the magnetisation curve of the AFM Heisenberg model in the classical limit[10]. In the context of spin models the classical limit means the limit of infinite spin length, $S \to \infty$. In this limit the spin operators of the Heisenberg Hamiltonian Eq. 20 become three-dimensional vectors, $S_i = S(\sin\theta_i \cos\varphi_i, \sin\theta_i \sin\varphi_i, \cos\theta_i)$ where θ_i, φ_i are the polar and azimuth angles, respectively, of the spin at site i. . Evidently the transitions in the ground state related to these cusps have their origin in the behaviour of the quantum system. This makes one wonder why most of the steps (i.e. quantum transitions caused by level crossings) in the zero-temperature magnetisation curve disappear in the classical limit, and why classical transition points can appear at different values of the applied field. We investigate this question by analysing the symmetries of the ground states of small AFM Heisenberg clusters and by extrapolating then these results to the classical limit[IV].

3.4.1 Computation of the symmetry of the ground state

The ground state of the AFM Heisenberg model with a fixed applied field B may or may not be degenerate depending on the dimension of the subspace related to the lowest eigenvalue for a fixed z component of the total spin S_z. With the symmetry of the ground state we mean the reduction of the subspace spanned by the ground state vectors into the direct sum of irreducible representations of the symmetry group of the system. The reduction process itself is a straightforward application of representation theory of finite groups[28]. Therefore only a short introduction to the subject is given here.

Let G be a (finite) group, V its representation and χ a character of the representation. To be precise V is a finite-dimensional vector space called the representation space and the representation itself is a homomorphism $\rho : G \to GL(V)$, where $GL(V)$ is a set of bijective linear maps from V to V. However, the representation ρ is commonly identified with the representation space V itself. From now on we also use this terminology. In general the representation space V has a reduction into a direct sum of the irreducible representations V_i of the group G,

$$V = \bigoplus_{i=1}^{k} a_i V_i \,, \tag{24}$$

where k equals the number of irreducible representations of group G and a_i gives the number of how many times the irreducible representation V_i appears in the reduction. The value of a_i is called the multiplicity, and is given by

$$a_i = \langle \chi | \chi_i \rangle = \frac{1}{N} \sum_{g \in G} \chi^*(g) \chi_i(g) \,. \tag{25}$$

Here N is the number of elements in the group and χ_i is the character of the irreducible representation V_i. Because the character is a class function, multiplicity a_i can be expressed as a sum over different classes $\mathcal{C}_j$ of group G

$$a_i = \frac{1}{N} \sum_{\mathcal{C}_j} c_j \chi(\mathcal{C}_j)^* \chi_i(\mathcal{C}_j) \,, \tag{26}$$

where c_j is the number of group elements in the class $\mathcal{C}_j$ and the sum is over all classes of the group G.

In the actual symmetry calculation group G is the symmetry group of the system. The representation space V is spanned by the eigenvectors of the lowest-lying eigenvalue corresponding to the fixed S_z. Therefore, in order to calculate multiplicity a_i using the Eq. 26, one must take one element from each class $\mathcal{C}_j$ and calculate its matrix representation in

the space V. Finally we note that the value of character χ at a point $g \in G$ is the trace of the matrix representation of $g \in G$ in space V, and thus it is enough to calculate only the diagonal elements of this matrix representation,

$$\chi(g) = \text{Trace}\,[\text{Mat}(g)] = \sum_{i=1}^{d} [\text{Mat}(g)]_{ii} \tag{27}$$

where d is the dimension of V.

Main results

About 15 years ago it became possible to measure magnetic properties of small clusters[29, 30]. Even before that some experiments had been made using granular samples[31]. In these earliest experiments it was however impossible to control the sizes of the grains and make a distinction between thermodynamical properties of the sample and the size distribution of the grains of the sample. However, a new era began in the beginning of the 90s when several experimental results were published for ferromagnetic transition metals (Fe and Co)[1, 2, 3]. Also theoretical results to explain the experimental findings were published[6, 7]. One of the most astonishing property found in these experiments was the increace of magnetisation as a function of temperature of small iron clusters within a considerable temperature range. However, there was some controversy as to the temperature determination of these clusters which was not properly settled.

At first theoretical intrest was concentrated on the ferromagnetic (FM) clusters (papers cited above), and experimental results were explained with the superparamagnetic (SPM) model, i.e. the clusters behave in an applied magnetic field as large paramagnetic spins. Also, the observed behaviour that the average magnetic moment of a cluster is smaller than the bulk value was interpreted through the SPM model. By assuming that thermal energy is larger than the anisotropy energy, a large magnetic moment can rotate almost freely with respect to the lattice, and the measured magnetic moment of the cluster is not the real moment but instead an average over its Boltzmann distribution. Taking this into account it was realised that the real average magnetic moments of the clusters are indeed larger than the bulk value. Later on interest turned to the properties of antiferromagnetic clusters which are in fact more complicated than those of their FM counterparts [9, I, II].

4 Antiferromagnetic Ising clusters

Depending on the size and geometry (lattice structure) of a cluster, it may be impossible to get a unique spin configuration which minimises the energy related to its magnetic degrees of freedom. This phenomenon is called frustration and it was shown to be one of the main features when explaining the magnetic properties of AFM Ising clusters[9, II]. Frustration means e.g. that when one goes around a closed loop along nearest neighbour pairs with spin directions such that the energies between each pair are minimised, then the energy of the final pair that includes the first spin cannot be minimised. The simplest system which has this property is a system of three spins in a triangular loop. In this system it is impossible to minimise the magnetic energies of all pairs at the same time. The frustrated spins that are free to change their direction without any cost in energy are responsible for the paramagnetic behaviour which can be observed at low temperatures and in low applied fields. In Ref. [9] only low values of the applied field and low temperatures were considered. Also, in this reference the Monte Carlo technique was used which becomes very slow at

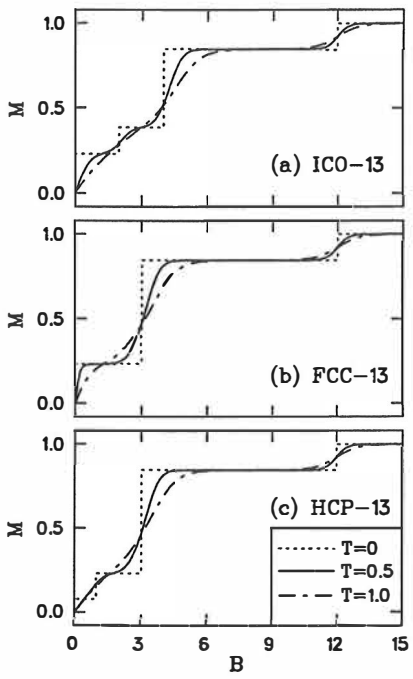

Figure 1: Magnetisation M as a function of applied field B for three Ising clusters of equal size (13 spins) but different lattice structure (ICO, FCC and HCP) are shown at three different temperatures, $T = 0, 0.5$ and $T = 1.0$.

low temperatures[32]. This is especially true for the AFM case where the ground state can be very complex. Therefore, in Refs. [I, II], a different kind of approach was chosen, and direct summation over all meaningful parts of the configuration space was used. A detailed description of the method is given in Ref. [33].

4.1 Superparamagnetic model and the AFM Ising clusters

At very low temperatures a step structure for the magnetisation curve M as a function of an applied field B is obtained (see Fig. 1). This results from competition between the applied field which tends to orient spins along the field direction, and the exchange interaction which favours antiparallel orientation between nearest neighbour spins. At higher temperatures these steps are rounded because, instead of one dominant state in the Boltzmann distribution as in the low temperature limit, the thermodynamical average at high temperatures of the magnetisation $M = M(B)$ has contributions from several different states.

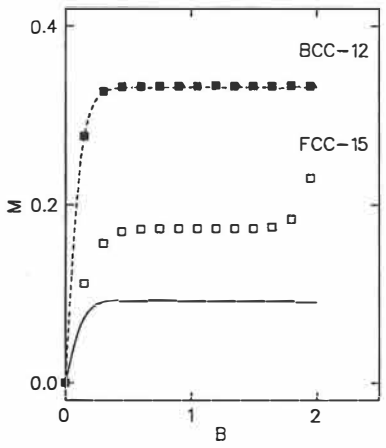

Figure 2: Magnetisation M as a function of applied field B of the clusters FCC-15 and BCC-12 at temperatures $T = 0.2$ and $T = 0.5$, respectively. Solid and dashed curves are obtained using the superparamagnetic model.

Because of the frustrated spins one might expect that the SPM model could be used also in the case of AFM Ising clusters. In general this is not however true except for certain cluster geometries and at very low temperatures and applied fields. Notice also that the applied field B and the temperature T are in units of the coupling constant J, which for instance for transition metals is supposed to be smaller in the AFM case than in the FM case[16]. In Fig. 2 we show the magnetisation curve M as a function of applied magnetic field B for two different lattice structures. It can be noticed from the Fig. 2 that clear deviation from an SPM type behaviour occurs in the case of the FCC-15 cluster even at the temperature $T = 0.2$, and practically for all values of the applied field. However, for the BCC-12 cluster the SPM model describes the magnetic behaviour considerably better. In low applied fields clear deviation from the predictions of the SPM model can be observed around the temperature $T = 1$.

For the AFM Ising clusters the SPM model fails mainly because of two reasons. Due to the AFM exchange interaction, the antiparallel spin alignment of nearest neighbours is favoured at low temperatures. Therefore the magnetisation of the ground state has a low value in a weak applied field B. On the other hand, the lowest-lying excited states have usually larger magnetic moments than the ground state, and thus a thermally excited single-spin flip can cause a relatively large increace in the magnetisation. Furthermore, the lowest lying excited states can have relatively high degeneracy, which also causes deviation from the SPM type behaviour.

These two reasons are also responsible for the anomalous behaviour of magnetisation

such that it increases for increasing temperature in a considerable temperature range. Therefore, when considering AFM Ising clusters, this surprising behaviour of the magnetisation M as a function of temperature has quite a simple explanation. Although bulk iron and cobalt are ferromagnetic, recent studies[43, III] indicate that it is possible the exchange coupling constatnt J_{ij} in Eq. 20 can change sign when the geometry and the average coordination number of the cluster varies. This means that a sign reversal of the exchange coupling constant J_{ij} might happen when the cluster size increases.

4.2 Clusters with incomplete shells

In earlier studies only clusters with complete shells and perfect symmetry were considered[9]. In this work we shall mean by a shell the geometric shell defined as a set of atoms whose distances from the center of the cluster are the same. To see if the picture based on the magnetic properties of clusters with complete shells is generic, clusters with incomplete shells were considered[I, II]. In the formation of real clusters the total energy is minimised. Because cohesion is the dominant part of the total energy of a cluster, we can neglect the magnetic energy contribution to it when determining the geometry of the cluster. Assuming further that nearest-neighbour interaction is the dominant part of cohesion, it is enough to maximise the number of the nearest-neighbour pairs in the cluster to determine its geometry. However, this is not a sufficient condition for a unique geometry of the cluster, and we also have to classify all geometrical isomers of the cluster and their degeneracy factors. By different geometrical isomers we mean different geometrical arrangements which cannot be transformed into each other by a symmetry operation of the underlying lattice structure. The symmetry group in the case of bcc and fcc clusters is the full symmetry group of the cube O_h. Therefore the thermodynamical averages e.g. magnetisation of the cluster are weighted averages over different geometrical configurations. As reported in Refs. [I, II], some new steps appear in the magnetisation curve $M = M(B)$ at low temperatures due to the geometrical isomers, but these disappear rapidly for increasing temperature. It was proposed by Reddy et al in Ref. [9] that the dependence of the magnetic properties on the geometry of the cluster could be used as an indirect method to define the lattice structure of the cluster. We demonstrated this explicitly for bcc and fcc lattice structures and cluster sizes $12 \leq N \leq 27$. The essential difference between the bcc and fcc clusters which is responsible for their different magnetic properties is that a spin in the bcc clusters has no nearest neighbours at the same shell. Therefore the effect of adding a new spin in the system adds up. This is not true for the fcc clusters where nearest-neighbour spins can be found at the same shell even in the small clusters considered in this thesis. This property introduces frustration into the fcc systems.

4.3 Clusters with locally modified coupling strengths

Motivation behind the modification of the coupling constants $\{J_{ij}\}$ is that small clusters do not necessarily have ideal lattice structure of any Bravais lattice[34, 35] because degeneracy can be reduced by lowering the symmetry of the system (the Jahn-Teller deformation). Magnetic interaction between the spins is related to overlap of the electron wave functions[16]. At the surface of a cluster this overlap is assumed to be smaller than in the bulk. Therefore we used a smaller coupling strength between the surface and core spins and investigated its effect on the magnetic properties of the cluster. The definition of a surface spin is somewhat arbitrary for the small clusters considered in this work. In this case we considered a spin as a surface spin if its coordination number was lower than the average coordination number of the cluster. Another modification was to randomise the interaction strengths J_{ij} using a binomial distribution. The final value for the magnetisation M is then a properly weighted average over the geometical isomers and a certain number of randomly picked realisations of $\{J_{ij}\}$.

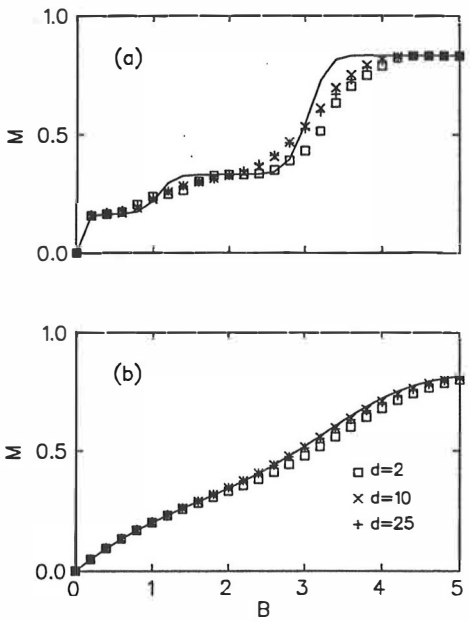

Figure 3: Magnetisation M as a function of applied field B of the FCC-12 cluster averaged over $d = 2, 10$ and 25 realisations of a set $\{J_{ij}\}$ compared with the magnetisation of the nonrandomised FCC-12 cluster (solid curve) at temperature (a) $T = 0.2$ and (b) $T = 1.0$.

As can be noticed from Fig. 3, magnetisation converges rapidly to that of the nonrandomised cluster when the number of realisations of $\{J_{ij}\}$ is increased. Although Fig. 3 only

shows results for FCC-12 with random realisations of $\{J_{ij}\}$, similar results were obtained also when the surface spins were weakly connected to the core spins.

These observations can be understood by using the results obtained in the previous section when several geometrical isomers were present. Any realisation of $\{J_{ij}\}$ can be interpreted as a geometrical isomer. In this case the number of possible geometrical forms is much larger than what had to be taken into account in the previous section. Furthermore, this interpretation of a random realisation of $\{J_{ij}\}$ as a geometrical isomer allows us to generalise the results obtained beyond the binomial distribution. Our results indicate that variations in the coupling constants J_{ij} of the cluster due to deviations from an idealised crystal structure, do not effect its magnetic propeties except at the lowest temperatures, and even then the effect is small.

5 Spin Hamiltonians for small Ni clusters

Recently spin Hamiltonians have been used in explaining the very long relaxation times measured for large magnetic molecules ($Mn_{12}Ac$)[25, 27, 36]. Quadratic and fourth order terms S_z^2, S_z^4 and $S_-^4 + S_+^4$ were proposed to be included in the spin Hamiltonian to explain experimental results.

As has been demonstrated in numerous investigations during the last few decades, magnetic, optical and electrical properties of clusters can undergo dramatic changes as a function of cluster size [37]. Despite the big practical and theoretical interest in these small systems, very little has been done to find the proper spin Hamiltonians for small assemblies of atoms. Some efforts have been made to compute spin Hamiltonian parameters using *ab initio* methods[17, 18]. In Ref. [III] a different kind of approach was used. Density-functional theory[11] in the local spin-density approximation (DFT-LSDA) was used to compute the electronic structure of small (Ni_3 and Ni_4) clusters. Having first solved the lowest-lying electronic levels and their magnetic moments, a suitably parametrised spin Hamiltonian which produces the DFT energy levels as accurately as possible, with correct values for the z component of the total spin, was constructed. In addition to the form of the spin Hamiltonian, also the length of individual spin was considered.

5.1 Computation of the electronic structure

Up to date most of the work has been concentrated on the determination of the magnetic moment per atom, and on how the local environment of an atom (coordination number, bond length) affects the magnetic properties of clusters[38, 39, 40, 41, 42]. Also, possible transitions between different magnetic phases (ferro-, para- and antiferromagnetic) have been of interest recently[43].

The electronic structure of small nickel clusters has previously been computed using several kinds of methods[38, 39, 40, 44]. We used the *ab initio* Born-Oppenheimer, local-spin-density-approximation (BO-LSDA) method devised by Barnett and Landman[45]. In the BO-LSDA method one solves the Kohn-Sham one-electron equations using the Kohn-Sham method explained in Sec. 2. The current procedure uses a plane wave basis combined with a nonlocal separable pseudopotential for the interaction of valence electrons with the ions. For the computation of the exchange-correlation energy in the LSDA approximation, we use the parametrisation of Vosko, Wilk and Nusair[46]. Only the outermost $3d$ and $4s$ orbitals were treated as valence orbitals, and the other orbitals as frozen core orbitals. Our DFT-LSDA results compare well with previous results for small nickel clusters[III]. For every cluster considered in this work the geometry was optimised for a fixed z component of the total spin. When the optimal geometry was reached, it was fixed, and the z component of the total spin was then allowed to relax to its optimal value (the ground state). Finally as many convergent electronic states as possible were computed using different values for the z component of the total spin and the optimised geometry for the cluster. Notice however that the total angular momentum of the cluster remains undetermined in the present DFT method because the orbital angular momentum $\boldsymbol{L}$ remains undetermined. Therefore only the z component of the total spin S_z due to the spins of the valence electrons is obtained.

For Ni_3 clusters two optimal geometries were found. However, only for the equilateral triangle several (4) fully converged electronic configurations with different S_z values were obtained. For the other geometry, the linear chain, only one fully converged spin state was obtained, and therefore it was impossible to find a suitably parametrised spin Hamiltonian for the linear Ni_3 cluster. For the Ni_4 cluster two optimal geometries, square and tetrahedron, were obtained with three fully converged electronic states. The results are shown in Table 5.1.

Table 5.1 The total energies E_{tot} (in eV) and the z components of the total spin S_z computed by the DFT-LSDA method for triangular Ni_3 and tetrahedron and square Ni_4 clusters.

Cluster	E_{tot}	S_z
Ni_3	0.000	1
	0.344	0
	0.350	2
	1.490	3
Ni_4 (tet)	0.000	2
	0.211	1
	0.309	0
Ni_4 (sq)	0.000	3
	0.098	2
	0.146	1

5.2 The form of the spin Hamiltonian for small Ni clusters

As already noted in the beginning of this Chapter, second and fourth order terms have quite recently been proposed to explain the magnetic properties of large magnetic molecules. There is a long tradition in using spin models to explain the magnetic properties of macroscopic systems[8]. As explained in Sec. 3.2, the Pauli exclusion principle causes the interactions of the electrons to depend on their spin quantum numbers. This leads to the exchange interaction which has its origin in the electrostatic interaction. Therefore, at least a Heisenberg type exchange interaction,

$$H_{ex} = \sum_{<i,j>} J_{ij}\mathbf{S}_i \cdot \mathbf{S}_j \,, \tag{28}$$

should be included in the effective spin Hamiltonian H_{eff}. Due to the inhomogeneous electric fields caused by the anisotropic electronic environment of the atoms, H_{ex} does not describe properly the magnetic behaviour of the cluster. Therefore, nonlinear single-site terms should also be included in this Hamiltonian. We thus assume that the effective spin Hamiltonian H_{eff} takes the form

$$H_{eff} = \sum_{<i,j>} J_{ij}\mathbf{S}_i \cdot \mathbf{S}_j + A\sum_{i=1}^{N}(S_i^z)^2 + C\sum_{i=1}^{N}(S_i^z)^3 + D\sum_{i=1}^{N}(S_i^z)^4 \,. \tag{29}$$

In the first term on the right hand side summation is over all nearest-neighbour pairs, and N is the number of spins (atoms) in the cluster. Notice also that the term $\sum_{i=1}^{N}(S_i^z)^3$ is included because small clusters do not necessarily have inversion symmetry that prevents the appearance of odd powers of S_i^z when describing the bulk magnetic properties. It is obvious e.g. that the equilater triangle and the tetrahedron do not have this symmetry. In all three clusters considered in this work all lattice sites are equivalent. Therefore the exchange constants J_{ij} have the same value for all couplings in a given cluster, and $J \equiv J_{ij}$ is used in all computations. For simplicity, at least one of the parameters A, C or D is set equal to zero. Because the z component of the total spin S_z is the only quantum number extracted from the DFT computations, the effective spin Hamiltonian H_{eff} must commute with S_z, i.e. $[H_{eff}, S_z] = 0$. Thus terms like $(S_i^+)^2 + (S_i^-)^2$ and $(S_i^+)^4 + (S_i^-)^4$ proposed in Ref. [26, 27] are not allowed to be included in the effective spin Hamiltonian H_{eff}. It has been shown before that the local environment of an atom has a profound influence on its magnetic properties[42, 43, 47], and that the total spin is reduced when increasing the number of nearest neighbours. Therefore, we use spin lengths $s = 1$ or $s = 2$ in the effective spin Hamiltonian, and exclude $s = 3$ and $s = 4$ obtained by Hund's rules for the lowest-lying electronic configurations $3d^9 4s^1$ and $3d^8 4s^2$, respectively. Notice also that the sign of the exchange coupling constant J is considered as a free parameter. As explained in Sec. 3.3 the real spin Hamiltonian can have terms of arbitrary orders and thus the effective spin Hamiltonian of Eq. 29 is only the beginning of a power series of spin operators of increasingly higher order.

5.3 The values of the spin Hamiltonian parameters for small Ni clusters

In each case the values for the fitting parameters A, C or D were determined by minimising the sum of squares

$$F = \sum_{i=2}^{c} [e_i^{DFT} - e_i^{SH}(A, C, D)]^2 , \tag{30}$$

of the differences between the spin Hamiltonian exitation energies $e_i^{SH}(A, C, D)$ and the DFT exitation energies e_i^{DFT} in the same spin state S_z; c equals the number of converged DFT electronic states. Possible solutions were also restricted by the constraint that the lowest-lying states have a z component of the total spin S_z consistent with the DFT result. A nonlinear optimisation NAG routine was used to solve this problem. To reduce the CPU time needed for the solution, the state space was split into subspaces in which $S_z = 0, 1, 2, \ldots$

If the optimisation routine failed to give a solution to the problem, the eigenvalue spectrum was computed on an interval $[-10, 10]$ in the one parameter case with a step length of 0.05, and on a square $[-10, 10] \times [-10, 10]$ in the two parameter case with a step length of 0.25 in each direction. For clusters which do not have inversion symmetry, i.e. Ni_3 and Ni_4 tedrahedron, C must be non-zero so that the effective spin Hamiltonian has the correct symmetry. For the same reason C must be zero for the Ni_4 square.

The best solutions to the nonlinear optimisation problem are shown in Table 5.3. For the tetrahedron we obtained perfect fits for spin lengths $s = 1$ and $s = 2$. On the other hand, the optimisation routine could not give a solution for the square, and the solution shown in Table 5.3 is obtained using a dense grid around the point where the nonlinear constraints were satisfied. As can be noticed from Table 5.3, the form of the optimal solution strongly depends on the geometry of the cluster. Even the signs of the exchange coupling constant J and the constant A can change with the geometry. This kind of transition between two different magnetic phases seems to be possible according to *ab initio* computations for nickel clusters[43]. This is plausible as the local environments of the atoms change considerably from cluster to cluster, and cause large changes in the local electron densities. This is especially true for the small clusters like Ni_3 and Ni_4 because in these systems all atoms can be considered as surface atoms. Notice also from the Table 5.3 that the higher order single site terms tend to dominate over the Heisenberg exchange interaction.

Table 5.3 The values of the parameters in the spin Hamiltonian giving the best fit to the computed DFT energy levels. s is the length of individual spin, sgn(J) gives the magnetic phase (FM, AFM) and A/J, C/J and D/J are the coefficients of the second, third and fourth order single-site terms, respectively.

Cluster	s	sgn(J)	A/J	C/J	D/J
Ni_3	1	-	2.158	1.536	0
Ni_4 (tet)	1	+	-1.086	1.368	0
Ni_4 (tet)	2	+	1.995	1.152	0
Ni_4 (sq)	2	-	-2.288	0	0.593

6 The classical limit of the AFM Heisenberg clusters

As explained in Section 3.2, under certain assumptions the magnetic interaction between two atoms can be described by the exchange of an electron pair between two atoms, and this leads to the Heisenberg type spin Hamiltonian. In an applied magnetic field B the Heisenberg Hamiltonian has the form of Eq. 21.

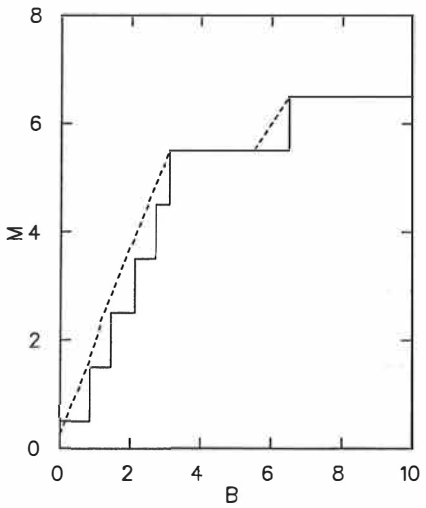

Figure 4: Magnetisation curves as a function of the applied field $M = M(B)$ for ICO-13 at zero temperature. Dashed curve is for the classical ICO-13 cluster and solid curve for the quantum case when $S = 1/2$.

In the numerical simulations of the classical AFM Heisenberg model Parkinson and Timonen found that at zero temperature the magnetisation curve $M = M(B)$ is a piecewise smooth function or a straight line[10]. In the quantum case this magnetisation curve $M = M(B)$ has a typical step structure at zero temperature. In Fig. 4 we show magnetisation curves at zero temperature of the ICO-13 cluster for both $S = 1/2$ and in the classical limit, i.e. for $S \to \infty$. Notice that in the classical system there are four transition points

(cusps on the $M = M(B)$ curve). This means that most of the steps in the quantum system disappear in the classical limit. Notice also that in the classical limit transitions can appear at different values of the applied field than in the quantum systems. Evidently these transition points have their origin in the behaviour of the quantum mechanical system. We have studied these questions by analysing the symmetries of the ground states of the AFM Heisenberg model. To obtain some characteristic features of the systems described by the AFM Heisenberg Hamiltonian, we have computed the lowest-lying eigenstates of the AFM Heisenberg Hamiltonian as a function of applied field B for several small clusters with different symmetries. Analysing the symmetries of the lowest-lying states and using as high spin values S as possible, it seems possible to extract some general features of these systems. For some systems we analysed the symmetries using an arbitrary spin length S and then extrapolated these results to the limit $S \to \infty$.

6.1 The periodicity of the symmetry of a spin-S pair

We start with the most simple case by considering a pair of spin-S atoms. Although this is almost trivial it illustrates the general features of most of the clusters. The Hamiltonian is now

$$\begin{aligned} \mathcal{H} &= \mathbf{s}_1 \cdot \mathbf{s}_2 - B(s_1^z + s_2^z) \\ &= \frac{1}{2}[(\mathbf{s}_1 + \mathbf{s}_2)^2 - \mathbf{s}_1^2 - \mathbf{s}_2^2] - B(s_1^z + s_2^z) \\ &= \frac{1}{2}[\mathbf{T}^2 - \mathbf{s}_1^2 - \mathbf{s}_2^2] - BT^z \\ &= \frac{1}{2}[T(T+1) - 2S(S+1)] - BM\,, \end{aligned} \tag{31}$$

where $\mathbf{T} = \mathbf{s}_1 + \mathbf{s}_2$. $T(T+1)$ is the eigenvalue of $\mathbf{T}^2$ and $T = 0, 1, 2, \ldots, 2S$. $M = T^z$ is the magnetisation of the cluster and so $-T \leq M \leq T$. The lowest energy for a given M is obtained for $T = M$. Crossover from M to $M+1$ occurs at B given by

$$\frac{1}{2}M(M+1) - BM = \frac{1}{2}(M+1)(M+2) - B(M+1)\,, \tag{32}$$

i.e. at $B = M + 1$. Thus the magnetisation curve is a series of steps of equal width 1 and height 1. To determine the symmetry of each of the states which occur at each step we note that a complete *basis* for the states with given M is the set $|q, M-q\rangle_b$ with $-T+M \leq q \leq T$. Subscript b indicates a basis state.

The space group of the pair is C_{2v} with two one-dimensional representations Γ_1, the trivial representation, and Γ_2. Provided $q \neq M - q$, the pair $|q, M-q\rangle_b, |M-q, q\rangle_b$ can be written in two linear combinations:

$$\frac{1}{\sqrt{2}}[|q, M-q\rangle_b + |M-q, q\rangle_b] \qquad \text{with symmetry } \Gamma_1 \tag{33}$$

and

$$\frac{1}{\sqrt{2}}[|q, M-q\rangle_b - |M-q, q\rangle_b] \qquad \text{with symmetry } \Gamma_2. \tag{34}$$

If $q = M - q$ then there is only a single state with symmetry Γ_1. Starting with the maximum $M = 2S$, there is only one state $|S, S\rangle_b$, so the symmetry is Γ_1. This is clearly an eigenstate with $T = 2S$, $M = 2S$ and energy $E = S^2 - 2BS$. Eigenstates will be written $|T, M\rangle$ without a subscript, so this is $|2S, 2S\rangle$. The subspace corresponding for the next highest $M = 2S - 1$ is two dimensional with the basis state vectors $|2S, 2S-1\rangle_b$ and $|2S-1, 2S\rangle_b$. Using these states it is possible to form two linear combinations with symmetries Γ_1 (symmetric) and Γ_2 (antisymmetric). The allowed values of T are $2S$ and $2S-1$, so the eigenstates will be $|2S, 2S-1\rangle$ and $|2S-1, 2S-1\rangle$. Since T is a good quantum number the first of these is obtained from $|2S, 2S\rangle$ by operating with the lowering operator $\mathbf{T}^-$ and must have the same symmetry Γ_1. The energy is $S^2 - B(2S-1)$. The other state, $|2S-1, 2S-1\rangle$ must have symmetry Γ_2 and it has a lower energy $S(S-2) - B(2S-1)$ since T is lower. In conclusion the step on the magnetisation curve with $M = 2S-1$ corresponds to a state with symmetry Γ_2.
If S is higher than $\frac{1}{2}$ the next highest state has $M = 2S - 2$. Otherwise there are no other steps (we consider only the case $B \geq 0$). The basis has three elements with symmetries Γ_1 (twice) and Γ_2 (once). Two of these have $T > M$ and are obtained from the two $M = 2S-1$ states by operating with $\mathbf{T}^-$ and have the same symmetries. The remaining state with $T = M$ has the lowest energy $S^2 - 4S + 1 - B(2S-2)$ and must have symmetry Γ_1. This is the symmetry of the $M = 2S - 2$ step.

Therefore when $M = 2S-n$ is reduced by one unit, the dimension of the corresponding subspace is increased by one. Depending on the value of n the new basis state, coming into play when n is increased by one, will be symmetric (Γ_1-state) if n is odd or antisymmetric (Γ_2-state) if n is even. This corresponds to a new eigenstate $|T_{\text{new}}, M_{\text{new}}\rangle$ with $T = M_{\text{new}} = M-n-1$. According to the Eq. 32 this is the lowest eigenstate corresponding to M_{new}. Thus the symmetry of the steps is alternating between Γ_1 and Γ_2 when M decreaces, starting with Γ_1 at the maximum $M = 2S$. The final step, for $B = 0$, $M = 0$, has symmetry Γ_1 for $2S$ even and Γ_2 for $2S$ odd. In the limit $S \to \infty$ the magnetisation steps become infinitesimal and the magnetisation curve becomes the straight line $M = B$ for $0 \leq B \leq 2S$, with $M = 2S$ for $B > 2S$. The symmetry is Γ_1 for $B > 2S$, but for $0 \leq B \leq 2S$ there is not a unique symmetry. Instead both Γ_1 and Γ_2 are present with equal weights. This result is, to our knowledge, the first full analysis of the symmetry of a *classical* magnetic system.

6.2 Equilateral triangle of spin-S atoms

Three spins arranged in an equilateral triangle with equal exchange between each pair have Hamiltonian

$$\begin{aligned}\mathcal{H} &= \mathbf{s}_1 \cdot \mathbf{s}_2 + \mathbf{s}_2 \cdot \mathbf{s}_3 + \mathbf{s}_3 \cdot \mathbf{s}_1 - B(s_1^z + s_2^z + s_3^z) \\ &= \frac{1}{2}[(\mathbf{s}_1 + \mathbf{s}_2 + \mathbf{s}_3)^2 - \mathbf{s}_1^2 - \mathbf{s}_2^2 - \mathbf{s}_3^2] - B(s_1^z + s_2^z + s_3^z)\end{aligned}$$

$$
\begin{aligned}
&= \frac{1}{2}[\mathbf{T}^2 - \mathbf{s}_1^2 - \mathbf{s}_2^2 - \mathbf{s}_3^2] - BT^z \\
&= \frac{1}{2}[T(T+1) - 3S(S+1)] - BM\,, \qquad (35)
\end{aligned}
$$

where $\mathbf{T} = \mathbf{s}_1 + \mathbf{s}_2 + \mathbf{s}_3$, $T = 0, 1, 2, \ldots, 3S$, and $-T \leq M \leq T$.

The symmetry group of equilateral triangle is the C_{3v}. The group has six elements and there are two one-dimensional irreducible representations Γ_1 and Γ_2 and one two-dimensional irreducible representation Γ_3[48]. Just as for the pair, the lowest state with a given M has $T = M$. Crossover from M to $M+1$ occurs at $B = M + 1$. A complete basis is the set $|a, b, c\rangle$ where a, b, c are the z components of the three spins. For a given M the requirement $a + b + c = M$ defines a plane with normal in the $(1, 1, 1)$ direction. The requirements $-S \leq a, b, c \leq S$ define a cube centred at the origin. The plane and the cube intersect to form a triangle with corners $(S, S, M - 2S)$, $(S, M - 2S, S)$ and $(M - 2S, S, S)$ provided $M \geq S$. For $0 \leq M \leq S$ the intersection is a six-sided figure with corners at $(S, -S, M)$ and its permutations. We need to find the number of points lying on each of these plane areas and their types. For conciseness we show only the states with $a \leq b \leq c$ explicitly in this Section.

For example for $S = 4$, $M = 7$ we have

$$
|-1, 4, 4\rangle \quad |0, 3, 4\rangle \quad |1, 2, 4\rangle \quad |1, 3, 3\rangle \quad |2, 2, 3\rangle\,, \qquad (36)
$$

and for $M = 6$

$$
|-2, 4, 4\rangle \quad |-1, 3, 4\rangle \quad |0, 2, 4\rangle \quad |0, 3, 3\rangle \quad |1, 1, 4\rangle \quad |1, 2, 3\rangle \quad |2, 2, 2\rangle\,. \qquad (37)
$$

For $M = 3$ we have

$$
\begin{array}{lllll}
|-4, 3, 4\rangle & |-3, 2, 4\rangle & |-3, 3, 3\rangle & |-2, 1, 4\rangle & |-2, 2, 3\rangle \\
|-1, 0, 4\rangle & |-1, 1, 3\rangle & |-1, 2, 2\rangle & |0, 0, 3\rangle & |0, 1, 2\rangle \\
|1, 1, 1\rangle\,. & & & & \qquad (38)
\end{array}
$$

A state with $a = b = c$ must have symmetry Γ_1. A state with $a = b \neq c$, or $a \neq b = c$, has three permutations which can be written in linear combinations with symmetries Γ_1 and Γ_3. A state with $a \neq b \neq c$ has six permutations with linear combinations with symmetries Γ_1, Γ_2 and $2 \times \Gamma_3$. (This combination forms the regular representation of the group C_{3v}.) Thus the complete basis for $S = 4$, $M = 7$, for example, has symmetries

$$
3(\Gamma_1 + \Gamma_3) + 2(\Gamma_1 + \Gamma_2 + 2\Gamma_3) = 5\Gamma_1 + 2\Gamma_2 + 7\Gamma_3\,,
$$

and for $M = 6$

$$
\Gamma_1 + 3(\Gamma_1 + \Gamma_3) + 3(\Gamma_1 + \Gamma_2 + 2\Gamma_3) = 7\Gamma_1 + 3\Gamma_2 + 9\Gamma_3\,.
$$

All the states with $M = 7$ have $T \geq 7$. Operating on each of these with $\mathbf{T}^-$ produces a state with the same symmetry and T but with $M = 6$. Consequently the symmetry of states with $T = M = 6$ is obtained by difference of the symmetries with $M = 7$ and $T = M = 6$,

$$2\Gamma_1 + \Gamma_2 + 2\Gamma_3.$$

Hence there are 7 states in all which form the $M = 6$ step of the magnetisation curve.

This method of finding the degeneracies and symmetries of each step is generalised to arbitrary S and arbitrary M (see Appendix A). The final result is as follows. For integer S and $M \leq S$ there is a cycle of 6 steps with the following symmetries

$$\begin{array}{ll} M = 6k & 2kZ + \Gamma_a \\ M = 6k+1 & 2kZ + \Gamma_b + \Gamma_3 \\ M = 6k+2 & 2kZ + \Gamma_a + 2\Gamma_3 \\ M = 6k+3 & 2kZ + \Gamma_a + 2\Gamma_b + 2\Gamma_3 \\ M = 6k+4 & 2kZ + 2\Gamma_a + \Gamma_b + 3\Gamma_3 \\ M = 6k+5 & 2kZ + \Gamma_a + 2\Gamma_b + 4\Gamma_3\,, \end{array} \tag{39}$$

where $\Gamma_a = \Gamma_1$, $\Gamma_b = \Gamma_2$ if S is even and $\Gamma_a = \Gamma_2$, $\Gamma_b = \Gamma_1$ if S is odd; $Z = \Gamma_1 + \Gamma_2 + 2\Gamma_3$.

For $S =$ integer $+\frac{1}{2}$ and $M \leq S$ there is a cycle of 3,

$$\begin{array}{ll} M = 3k + \frac{1}{2} & \Gamma_1 + \Gamma_3 + kZ \\ M = 3k + \frac{3}{2} & \Gamma_1 + \Gamma_2 + \Gamma_3 + kZ \\ M = 3k + \frac{5}{2} & (k+1)Z\,. \end{array} \tag{40}$$

For $M \geq S$, putting $M = 3S - n$, the sequence for all S is

$$\begin{array}{ll} n = 6k & kZ + \Gamma_1 \\ n = 6k+1 & kZ + \Gamma_3 \\ n = 6k+2 & kZ + \Gamma_1 + \Gamma_3 \\ n = 6k+3 & kZ + \Gamma_1 + \Gamma_2 + \Gamma_3 \\ n = 6k+4 & kZ + \Gamma_1 + 2\Gamma_3 \\ n = 6k+5 & (k+1)Z\,. \end{array} \tag{41}$$

For large S the steps have massive degeneracy. This is mainly due to the large number of representations which are present at each step. When S is very large and M is not equal to 0 or $3S$, the dominant feature is a multiple of Z. This is to be expected since the vast majority of states will have $a \neq b \neq c$. Therefore we conjecture that the symmetry in the classical limit is given by $Z = \Gamma_1 + \Gamma_2 + 2\Gamma_3$ when $M \neq 0, 1$ in which magnetisation for the totally magnetised system is normalised to the unity. These results have been checked numerically for many different S.

6.3 Square of spin-S atoms

Square of four spins with equal exchange between each nearest-neighbour pairs have Hamiltonian

$$\begin{aligned}\mathcal{H} &= \mathbf{s}_1\cdot\mathbf{s}_2+\mathbf{s}_2\cdot\mathbf{s}_3+\mathbf{s}_3\cdot\mathbf{s}_4+\mathbf{s}_4\cdot\mathbf{s}_1-B(s_1^z+s_2^z+s_3^z+s_4^z)\\ &= (\mathbf{s}_1+\mathbf{s}_3)\cdot(\mathbf{s}_2+\mathbf{s}_4)-B(s_1^z+s_2^z+s_3^z+s_4^z)\\ &= \mathbf{t}_1\cdot\mathbf{t}_2-B(t_1^z+t_2^z)\,,\end{aligned}\tag{42}$$

where $\mathbf{t}_1=\mathbf{s}_1+\mathbf{s}_3$ and $\mathbf{t}_2=\mathbf{s}_2+\mathbf{s}_4$. This behaves as a pair of coupled spins with not necessarily equal length. In fact $t_1,t_2=0,1,\ldots,2S$, and

$$\begin{aligned}\mathcal{H} &= \frac{1}{2}[(\mathbf{t}_1+\mathbf{t}_2)^2-\mathbf{t}_1^2-\mathbf{t}_2^2]-B(t_1^z+t_2^z)\\ &= \frac{1}{2}[\mathbf{T}^2-\mathbf{t}_1^2-\mathbf{t}_2^2]-BT^z\\ &= \frac{1}{2}[T(T+1)-t_1(t_1+1)-t_2(t_2+1)]-BM\,,\end{aligned}\tag{43}$$

where $\mathbf{T}=\mathbf{t}_1+\mathbf{t}_2$; $T(T+1)$ is the eigenvalue of $\mathbf{T}^2$ and $M=T^z$.

For a given T and M the lowest energy is obtained by choosing the largest values for t_1,t_2, namely $t_1=t_2=2S$. All values of $0\le T\le 4S$ can be obtained with this choice. For a given M the lowest energy state has $T=M$ so the energy is

$$E=-\frac{1}{2}[M(M+1)-4S(2S+1)]-BM\,.\tag{44}$$

The situation is now identical to that of two spin-$2S$ atoms and so the degeneracies and the symmetries are almost similar than what was obtained in Section 6.1. However, the symmetries of these states are those of the group C_{2v}, whereas the space group of the square is C_{4v}.

The relation between the irreducible representations of a group C_{4v} and a subgroup C_{2v} are in general rather complex. However, in our numerical studies of finite S for this system we found that the representations of the relevant states alternated between Γ_1 and Γ_4 in the same way as the representations of the relevant states for the pair of spins alternated between Γ_1 and Γ_2. We therefore believe that for all S the magnetisation steps of the square have representation Γ_1 if M is even and Γ_4 if M is odd. Thus the symmetry in the classical limit should be described by Γ_1 and Γ_4 with equal weights. Notice however that we have not proved that the symmetry is alternated between Γ_1 and Γ_4 for general S as was done for the pair of S-spins.

6.4 5-atom ring of spin-S atoms

The group in this case is C_{5v}. The Hamiltonian is

$$\begin{aligned}\mathcal{H} &= \mathbf{s}_1\cdot\mathbf{s}_2+\mathbf{s}_2\cdot\mathbf{s}_3+\mathbf{s}_3\cdot\mathbf{s}_4+\mathbf{s}_4\cdot\mathbf{s}_5+\mathbf{s}_5\cdot\mathbf{s}_1\\ &\quad -B(s_1^z+s_2^z+s_3^z+s_4^z+s_5^z)\,.\end{aligned}\tag{45}$$

This Hamiltonian cannot be factorised in the same way as the previous ones, so we cannot obtain the symmetries for general S. Our numerical calculations on finite $S\le\frac{5}{2}$ systems show the following pattern. For $M=5S-n$, the representation r is given by

$$\begin{array}{cccccccccccccc} n & 0 & 1 & 2 & 3 & 4 & 5 & 6 & 7 & 8 & 9 & 10 & 11 & 12\\ r & \Gamma_1 & \Gamma_4 & \Gamma_3 & \Gamma_3 & \Gamma_4 & \Gamma_2 & \Gamma_4 & \Gamma_3 & \Gamma_3 & \Gamma_4 & \Gamma_1 & \Gamma_4 & \Gamma_3\,. \end{array}\tag{46}$$

Unfortunately dimensions of subspaces with definite M increase rapidly when S is increaced and it is impossible to obtain correct period of the ground state symmetries using numerical methods only. However, the pattern of period 10 when repeating indefinitely would be consistent for the numerical results we have obtained so far.

6.5 Tetrahedron

The group is the tetrahedral group T_d with 24 elements. There are two 1-dimensional irreducible representations Γ_1 and Γ_2, one 2-dimensional irreducible representation Γ_3 and two 3-dimensional irreducible representations Γ_4 and Γ_5[48]. Each atom has three neighbours and the Hamiltonian is

$$\begin{aligned}\mathcal{H} &= \mathbf{s}_1\cdot\mathbf{s}_2+\mathbf{s}_1\cdot\mathbf{s}_3+\mathbf{s}_1\cdot\mathbf{s}_4+\mathbf{s}_2\cdot\mathbf{s}_3+\mathbf{s}_3\cdot\mathbf{s}_4+\mathbf{s}_4\cdot\mathbf{s}_2\\ &\quad -B(s_1^z+s_2^z+s_3^z+s_4^z)\\ &= \frac{1}{2}[(\mathbf{s}_1+\mathbf{s}_2+\mathbf{s}_3+\mathbf{s}_4)^2-\mathbf{s}_1^2-\mathbf{s}_2^2-\mathbf{s}_3^2-\mathbf{s}_4^2]\\ &\quad -B(s_1^z+s_2^z+s_3^z+s_4^z)\\ &= \frac{1}{2}[\mathbf{T}^2-4S(S+1)]-BT^z\\ &= \frac{1}{2}[T(T+1)-4S(S+1)]-BM\,,\end{aligned}\tag{47}$$

where $\mathbf{T}=\mathbf{t}_1+\mathbf{t}_2+\mathbf{t}_3+\mathbf{t}_4$ and $0\le T\le 4S$. The lowest state for a given M has $T=M$.

For a given M the basis states of the form $|a,b,c,d\rangle$ have $a+b+c+d=M$ which defines a 'plane' in $4D$ space which intersects a hypercube defined by $-S \le a,b,c,d \le S$. For $2S \le M \le 4S$ the intersection is a tetrahedron with four vertices given by $(S,S,S,M-3S)$ and its permutations. For $0 \le M \le 2S$ the intersection is a truncated tetrahedron with 12 vertices given by $(S,S,-S,M-S)$ and its permutations, which becomes a regular octahedron at $M=0$. We have not analysed this situation in the same way as for the triangle, but the numerical results for $S \le \frac{5}{2}$ show the following pattern.

For $2S \le M \le 4S$ with $M = 4S-n$ the representations r are

$$\begin{array}{cl} n & r \\ 0 & \Gamma_1 \\ 1 & \Gamma_1+\Gamma_3+\Gamma_5 \\ 2 & \Gamma_1+\Gamma_4+2\Gamma_5 \\ 3 & 2\Gamma_1+2\Gamma_3+\Gamma_4+2\Gamma_5 \\ 4 & \Gamma_1+\Gamma_3+2\Gamma_4+4\Gamma_5\,. \end{array} \tag{48}$$

For $0 \le M \le 2S$ we do not have sufficient numerical data to identify a regular pattern. Note however that the basis state $|a,b,c,d\rangle$ with $a \ne b \ne c \ne d$ and its 24 permutations form a set of states with symmetry (the regular representation of T_d)

$$Z = \Gamma_1+\Gamma_2+2\Gamma_3+3\Gamma_4+3\Gamma_5\,. \tag{49}$$

For large S this combination will dominate the overall symmetry of the massively degenerate steps in the magnetisation curve. Therefore symmetry in the classical limit should be characterised by the Z whenever the system is not fully magnetised or $M \ne 0$.

6.6 Octahedron

The group is O_h with 48 elements. There are four irreducible representations, Γ_1^+, Γ_2^+, Γ_1^- and Γ_2^-, of dimension 1. There are two, Γ_3^+ and Γ_3^-, of dimension 2, and there are four, Γ_4^+, Γ_5^+, Γ_4^- and Γ_5^-, of dimension 3[48].

In this case the Hamiltonian is

$$\begin{aligned} \mathcal{H} &= (\mathbf{s}_1+\mathbf{s}_6)\cdot(\mathbf{s}_2+\mathbf{s}_3+\mathbf{s}_4+\mathbf{s}_5) \\ &\quad +\mathbf{s}_2\cdot\mathbf{s}_3+\mathbf{s}_3\cdot\mathbf{s}_4+\mathbf{s}_4\cdot\mathbf{s}_5+\mathbf{s}_5\cdot\mathbf{s}_2 \\ &\quad -B(s_1^z+s_2^z+s_3^z+s_4^z+s_5^z+s_6^z) \\ &= \mathbf{t}_1\cdot\mathbf{t}_2+\mathbf{t}_2\cdot\mathbf{t}_3+\mathbf{t}_3\cdot\mathbf{t}_1-B(t_1^z+t_2^z+t_3^z)\,, \end{aligned} \tag{50}$$

where $\mathbf{t}_1=\mathbf{s}_1+\mathbf{s}_6$, $\mathbf{t}_2=\mathbf{s}_2+\mathbf{s}_4$ and $\mathbf{t}_3=\mathbf{s}_3+\mathbf{s}_5$. This is not exactly the Hamiltonian of the triangle discussed earlier because the lengths of the three spins do not have to be equal. Hence

$$\begin{aligned}\mathcal{H} &= \frac{1}{2}[(\mathrm{t}_1+\mathrm{t}_2+\mathrm{t}_3)^2-\mathrm{t}_1^2-\mathrm{t}_2^2-\mathrm{t}_3^2]-B(t_1^z+t_2^z+t_3^z)\\ &= \frac{1}{2}[\mathrm{T}^2-\mathrm{t}_1^2-\mathrm{t}_2^2-\mathrm{t}_3^2]-BT^z\\ &= \frac{1}{2}[T(T+1)-t_1(t_1+1)-t_2(t_2+1)-t_3(t_3+1)]-BM\,, \end{aligned} \tag{51}$$

where $\mathbf{T}=\mathrm{t}_1+\mathrm{t}_2+\mathrm{t}_3$; T, t_1, t_2 and t_3 are the lengths of the combined spins $\mathbf{T}$, t_1, t_2 and t_3, respectively, so that $0\le t_1,t_2,t_3\le 2S$, $T_{min}\le T\le t_1+t_2+t_3$. T_{min} is the smallest length that can be formed from the three spins t_1, t_2 and t_3. $M=T^z$ so $-T\le M\le T$. From Eq. 51 it is clear that the lowest energy for a given M will be obtained by choosing the largest values for t_1, t_2 and t_3, namely $t_1=t_2=t_3=2S$. With this choice the Hamiltonian becomes the same as for the triangle and so the earlier results will apply, replacing S by $2S$.

The symmetry of the relevant states for the triangle are in terms of the irreducible representations of C_{3v}. The relation between these and the corresponding states of the octahedron is not simple to prove. However, in all our numerical studies we find that the relevant states of the octahedron have symmetries in which the Γ_a of C_{3v} is replaced by Γ_a^+ of O_h. Of course states with symmetry Γ_a^- do occur but these are never the lowest for a given M and so do not have any effect on the zero-temperature magnetisation curve. The cycles of length 3 or 6 seen for the triangle are seen in exactly the same way for the octahedron as for the triangle.

6.7 FCC-12 and ICO-12 clusters

The magnetic behaviour of these large clusters using finite spin length S and their classical limit were investigated in Ref. [10]. The ICO-12 is particularly interesting because there appear to be two distinct regions of the magnetisation curve. We have obtained the symmetries of the low-lying states for $S=\frac{1}{2}$ only. For FCC-12 the symmetry group is O_h and the symmetries r are

$$\begin{array}{cccccccc} M & 0 & 1 & 2 & 3 & 4 & 5 & 6 \\ r & \Gamma_1^- & \Gamma_5^- & \Gamma_1^+ & \Gamma_1^+ & \Gamma_1^+ + \Gamma_3^+ & \Gamma_3^+ + \Gamma_5^- & \Gamma_1^+ . \end{array} \tag{52}$$

For ICO-12 the group is I_h and the symmetries are

$$\begin{array}{cccccccc} M & 0 & 1 & 2 & 3 & 4 & 5 & 6 \\ r & \Gamma_3^+ & \Gamma_5^- & \Gamma_4^- & \Gamma_5^+ & \Gamma_3^- & \Gamma_1^+ & \Gamma_1^+ . \end{array} \tag{53}$$

For $S=1$ we obtained only a few results for high M, and found that the symmetries of the states with $M=12S-n$ for $n=0,1,2,3,4$ were the same as for $S=\frac{1}{2}$.

Clusters with an additional central atom, FCC-13 and ICO-13, show exactly the same symmetries except for one or more additional steps with Γ_1^+ symmetry at large M. The number of these additional steps seems to be equal to $2S$.

The number of steps for all these clusters is too small to determine a pattern which would apply at general S and would enable symmetry of the different regions of the classical curve to be described. This is due to the fact that the dimension of a subspace for definite M increases rapidly when the length of a spin S is increased. This makes the problem hard to solve numerically.

6.8 Conclusion

For quantum spin systems with small numbers of spins arranged in clusters with high symmetry, it is possible to categorise the ground state wave function in a magnetic field in terms of the irreducible representations of the space group of the cluster. We have shown, for certain of these clusters, how to obtain the complete decomposition of the states in terms of these representations for arbitrary spin S. Sometimes a single irreducible representation is present, although of course if this has dimension greater than one there will be degeneracy. Sometimes several representations are present giving additional degeneracy. Sometimes massive degeneracy occurs, of the order of NS, due to the fact that some representations occur several times, although some do not occur at all.

The fact that our results are for arbitrary S means that the *classical* ground states ($S \to \infty$) can be studied. We find that, even if the quantum states belong to a single irreducible representation, the representations varies in a systematic way as the applied field changes so that the classical system cannot normally be described by a single representation. Clearly this is even more true in the case when a quantum system has degeneracies between states of different irreducible representations. For some clusters the dominant representation is the combination of irreducible representations known as the regular representation. The numerical results indicate that this is the case if topology of the cluster is of definite type namely if every spin is connected to all other spins.

In the quantum case when the symmetry of the lowest lying state changes there is a step in the magnetisation curve $M = M(B)$. If the limiting prosess $S \to \infty$ is smooth the same could be true also in the classical system, i.e. when the classical symmetry changes there is a cusp in the magnetisation curve $M = M(B)$. The remaining question is how to generalise group theoretical concepts related to the finite dimensional space (with finite S) to the infinite dimensional case related to the classical limit. If the symmetry is periodic or quasiperiodic it seems reasonable that the classical symmetry is somehow related to the properly normalised sum of the irreducible representations over the period or quasiperiod. For instance, for OCT-6 there are two different periods, the one when $M \leq 2S$ and the other when $M \geq 2S$. However, the sums of irreducible representations over the periods are the same both below and above $M = 2S$. Notice also that the classical magnetisation curve

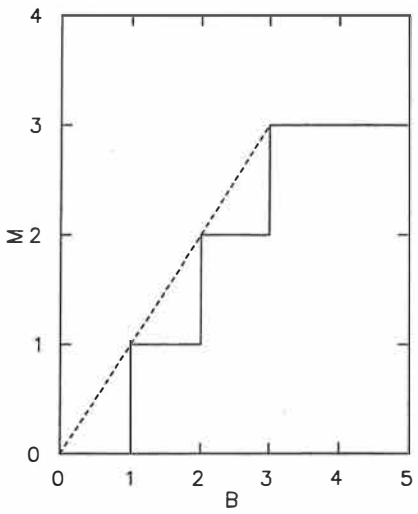

Figure 5: Magnetisation M for octahedral (OCT-6) as a fucntion of applied field B. Dashed line is for the classical system and solid curve for the quantum case when $S = 1/2$.

$M = M(B)$ is a straight line as it should if the limiting prosess is smooth (see Fig. 5).

Unfortunately we were not able to fully analyse any system in which the classical magnetisation curve $M = M(B)$ would have been a piecewise smooth curve to see if the classical symmetry is related to the sum of irreducible representations over the period (quasiperiod) as described above. Nevertheless, assuming that the classical symmetry is related to the sum of irreducible representations over the period (quasiperiod) and that the transition occurs when the periodicity changes in such a way that the sum of irreducible representations over the two periods have different values, then it is easy to understand why a cusp in the classical magnetisation curve does not appear at the same value of the applied field as for the finite spin length S.

7 Summary

The magnetic properties of small antiferromagnetic clusters were studied using the Ising model with nearest neighbour interactions and direct summation over the state space. It was observed that the superparamagnetic model, which has been used to explain experimental results for small ferromagnetic clusters, cannot in general explain the magnetic behaviour of small AFM Ising clusters. We also demonstrated that magnetic properties of these clusters are rather insensitive to variations in the exchange coupling constant. The effect of lattice

structure on the magnetic properties of the clusters was found to be so strong that the latter could be used as an indirect method for determining the lattice structure.

Density functional theory was used to compute lowest-lying electronic states of small nickel clusters. Then a suitably parametrised spin Hamiltonian was fitted to this energy spectrum. The parameters of the spin Hamiltonian were found to strongly depend on cluster geometry and on the number of spins in the cluster, including the sign of the exchange coupling constant.

Group theoretical methods were finally used to investigate the zero-temperature magnetic transitions of antiferromagnetic Heisenberg clusters in the classical limit. For the first time the magnetic symmetry of classical AFM Heisenberg sustem was obtained, and a suggestion to define this symmetry generally in the classical limit was made. Also, a sufficient condition was conjectured for a zero-temperature phase transition to occur in the classical limit.

A Appendix

In this Appendix we give the details of the symmetries of the lowest states for a triangle of spin S-atoms. As noted there are two distinct regions depending whether M is less than or greater than S.

First the region $M \leq S$. The plane area bounded by the six corners $(S, -S, M)$ and its permutations contains a total of

$$N_T = 3S(S+1) - M^2 + 1 \tag{54}$$

states. Let the number of states of the form (a, a, a) be N_3, of the form (a, a, b) with $b \neq a$ (and permutations) be N_2, and of the form (a, b, c) with $a \neq b \neq c$ be N_1. Clearly $N_3 = 1$ if $2M$ is divisible by 3 and $N_3 = 0$ otherwise. For states of the form (a, a, b) we have $2a+b = M$ and $-S \leq b \leq S$, so

$$-A_1 \leq a \leq A_2\,, \tag{55}$$

where

$$A_1 = \frac{S-M}{2} \text{ and } A_2 = \frac{S+M}{2}\,. \tag{56}$$

The minimum value of a will be equal to $-A_1$ if $S-M$ is even and the maximum will be equal to A_2 if $S+M$ is even. If S is an integer and both $S-M$ and $S+M$ are even then the number of values of a is $N_a = S+1$. If S is an integer and both $S-M$ and $S+M$ are odd then $N_a = S$. If S is an integer plus $\frac{1}{2}$ then one of $S-M$ and $S+M$ is even and one odd. In this case is $N_a = S + \frac{1}{2}$. States of the form (a, a, b) have three permutations unless $b = a$, so

$$N_2 = 3(N_a - N_3)\,. \tag{57}$$

Finally

$$N_1 = N_T - N_2 - N_3\,. \tag{58}$$

For integer S the alternation between even and odd values of N_a for successive values of M and the cycle of 3 in N_3, resulting in a cycle of 6 overall. For integer plus $\frac{1}{2}$ the cycle is length 3.

The symmetries of the states for a given M are given by

$$X_M = N_3(\Gamma_1) + \frac{1}{3}N_2(\Gamma_1 + \Gamma_3) + \frac{1}{6}N_1(\Gamma_1 + \Gamma_2 + 2\Gamma_3)\,. \tag{59}$$

The symmetries of the lowest states of a given M are those for which $T = M$ and these are given by $X_M - X_{M+1}$.

The final result is:

For $S =$ integer $+\frac{1}{2}$,

$$\begin{array}{ll} M = 3k + \frac{1}{2} & \Gamma_1 + \Gamma_3 + kZ \\ M = 3k + \frac{3}{2} & \Gamma_1 + \Gamma_2 + \Gamma_3 + kZ \\ M = 3k + \frac{5}{2} & (k+1)Z\,, \end{array} \tag{60}$$

where $0 \leq k \leq S/3$, $Z = \Gamma_1 + \Gamma_2 + 2\Gamma_3$.

For $S =$ even integer,

$$\begin{array}{ll} M = 6k & 2kZ + \Gamma_1 \\ M = 6k+1 & 2kZ + \Gamma_2 + \Gamma_3 \\ M = 6k+2 & 2kZ + \Gamma_1 + 2\Gamma_3 \\ M = 6k+3 & 2kZ + \Gamma_1 + 2\Gamma_2 + 2\Gamma_3 \\ M = 6k+4 & 2kZ + 2\Gamma_1 + \Gamma_2 + 3\Gamma_3 \\ M = 6k+5 & 2kZ + \Gamma_1 + 2\Gamma_2 + 4\Gamma_3\,. \end{array} \tag{61}$$

For $S =$ odd integer the result is the same as for even integer except that Γ_1 and Γ_2 are interchanged.

Now consider the region $S \geq M \geq 3S$. The plane region bounded by the corners $(S, S, M - 2S)$ and its permutations contains a total of

$$N_T = \frac{1}{2}(3S - M + 1)(3S - M + 2) \tag{62}$$

states. Again $N_3 = 1$ if $2M$ is divisible by 3 and $N_3 = 0$ otherwise.

States of the form (a, a, b) occur for $M - 2S \leq b \leq S$ and so

$$\frac{M - S}{2} \leq a \leq S. \tag{63}$$

Hence, $N_a = \frac{1}{2}(3S - M) + 1$ if $M - S$ is even and $N_a = \frac{1}{2}(3S - M)$ if $M - S$ is odd.

Here there is a cycle of length 6 for all S. The symmetries are

$$
\begin{array}{ll}
M = 3S - 6k & kZ + \Gamma_1 \\
M = 3S - 6k - 1 & kZ + \Gamma_3 \\
M = 3S - 6k - 2 & kZ + \Gamma_1 + \Gamma_3 \\
M = 3S - 6k - 3 & kZ + \Gamma_1 + \Gamma_2 + \Gamma_3 \\
M = 3S - 6k - 4 & kZ + \Gamma_1 + 2\Gamma_3 \\
M = 3S - 6k - 5 & (k+1)Z\,.
\end{array}
\tag{64}
$$

References

[I] **Properties of small antiferromagnetic Ising clusters**
E. Viitala, J. Merikoski, M. Manninen and J. Timonen
Z. Phys. D **40**, 173 (1997).

[II] **Antiferromagnetic order and frustration in small clusters**
E. Viitala, J. Merikoski, M. Manninen and J. Timonen
Phys. Rev. B **55**, 11541 (1997).

[III] **Spin Hamiltonians for small Ni clusters**
E. Viitala, H. Häkkinen, M. Manninen and J. Timonen
Phys. Rev. B, in press.

[IV] **Quantum to classical transition for small magnetic cluster in an external magnetic field**
J. B. Parkinson, R. J. Elliot, E. Viitala and J. Timonen
To be published.

[1] W. A. de Heer, P. Milani and A. Châtelain, Phys. Rev. Lett. **65**, 488 (1990).

[2] J. P. Bucher and L. A. Bloomfield, Int. J. Mod. Phys. B **7**, 1079 (1993).

[3] I. M. L. Billas, J. A. Becker and W. A. de Heer, Z. Phys. D **26**, 325 (1993).

[4] S. E. Apsel, J. W. Emmert, J. Deng and L. A. Bloomfield, Phys. Rev. Lett. **76**, 1441 (1996).

[5] W. Gerlach and O. Stern, Z. Phys. **8**, 110 (1922).

[6] S. N. Khanna and S. Linderoth, Phys. Rev. Lett. **67**, 742 (1991).

[7] J. Merikoski, J. Timonen and M. Manninen, Phys. Rev. Lett. **66**, 938 (1991).

[8] G. T. Rado and H. Suhl, *Magnetism Vol. II B* (Academic Press, New York and London 1966).

[9] B. V. Reddy and S. N. Khanna, Phys. Rev. B **45**, 10103 (1992).

[10] J. P. Parkinson and J. Timonen, to be published.

[11] P. Hohenberg and W. Kohn, Phys. Rev. **136**, 864 (1964).

[12] W. Kohn and L. J. Sham, Phys. Rev. **140**, 1133 (1965).

[13] R. G. Parr and W. Yang, *Density-Functional Theory of Atoms and Molecules* (Oxford University Press, New York, 1989).

[14] G. Vignale and M. Rasolt, Phys. Rev. B **37**, 10685 (1988).

[15] J. Hubbard, Proc. Roy. Soc. Lond. A **276**, 238 (1963); *ibid* A **281**, 401 (1964).

[16] N. W. Ashcroft and N. D. Mermin, *Solid State Physics* (Holt, Rinehart and Winston, New York, 1976); D. C. Mattis, *The Theory of Magnetism Vol. I and Vol. II* (Springer, Berlin, 1981).

[17] F. Illas, J. Casanovas, M. A. García-Bach, R. Caballol and O. Castell, Phys. Rev. Lett. **71**, 3549 (1993).

[18] M. S. S. Brooks, O. Eriksson, J. M. Wills and B. Johansson, Phys. Rev. Lett. **79**, 2546 (1997).

[19] W. Heitler and F. London, Z. Physik **44**, 455 (1927).

[20] P. A. M. Dirac, Proc. Roy. Soc. **A123**, 714 (1929).

[21] J. H. Van Vleck, Phys. Rev. **45**, 405 (1934).

[22] C. Møller, Z. Physik **82**, 559 (1933).

[23] E. Ising, Z. Phys. **31**, 253 (1925).

[24] W. J. Caspers, *Spin Systems* (World Scientific, Singapore, 1989).

[25] J. Villain, F. Hartman-Boutron, R. Sessoli and A. Rettori, Europhys. Lett. **27**, 159 (1994).

[26] P. Politi, A. Rettori, F. Hartman-Boutron and J. Villain, Phys. Rev. Lett. **75**, 537 (1995).

[27] A. Fort, A. Rettori, J. Villain, D. Gatteschi and R. Sessoli, Phys. Rev. Lett. **80**, 612 (1998).

[28] A. W. Joshi, *Elements of Group Theory for Physicists* (Wiley Eastern, New Delhi, 1973); M. Tinkham, *Group Theory and Quantum Mechanics* (McGraw-Hill Book Company, New York, 1964).

[29] T. D. Mark and A. W. Castleman, Adv. At. Mol. Phys. **20**, 65 (1985).

[30] D. M. Cox, D. J. Trevor, R. L. Whetten, E. A. Rohlfing and A. Kador, Phys. Rev. B **32**, 7290 (1985).

[31] E. F. Kneller and F. E. Luborsky, J. Appl. Phys. **34**, 656 (1963).

[32] D. W. Heermann, *Computer Simulation Methods in Theoretical Physics* (Springer, Berlin 1986).

[33] Juha Merikoski, Ph.D.Thesis, Dept. of Phys., Univ. of Jyväskylä, Research Report 1/94 (1994).

[34] B. Piveteau, M-C. Desjonquéres, A. M. Olis and D. Spanjaard, Phys. Rev. B **53**, 9351 (1996).

[35] F. A. Reuse, S. N. Khanna and S. Bernel, Phys. Rev. B **52**, 11650 (1995).

[36] A. L. Barra, D. Gatteschi and R. Sessoli, Phys. Rev. B **56**, 8192 (1997).

[37] J. Bernholc *Physics Today*, Sep. 1999.

[38] J. L. Rodrígues-López, F. Aguileira-Granja, A. Vega and J. A. Alonso, Eur. Phys. J. D **6**, 235 (1999).

[39] F. A. Reuse and S. N. Khanna, Chem. Phys. Lett. **234**, 77 (1995).

[40] N. Fujima and T. Yamaguchi, Phys. Rev. B **54**, 26 (1996).

[41] J. Guevara, F. Parisi, A. M. Llois and M. Weissmann, Phys. Rev. B **55**, 13283 (1997).

[42] P. J. Jensen and K. H. Bennemann **Z**. Phys. D **35**, 273 (1995).

[43] E. Munõz-Sandoval, J. Dorantes-Dávilla and G. M. Pastor, Eur. Phys. J. D **5**, 89 (1999).

[44] M. Tomonari, H. Tatewaki and T. Nakamura, J. Chem. Phys. **85**, 2875 (1986).

[45] R. N. Barnett and U. Landman, Phys. Rev. B **48**, 2081 (1993).

[46] S. H. Vosko, L. Wilk and M. Nusair, Can. J. Phys. **58**, 1200 (1980); S. H. Vosko and L. Wilk, J. Phys. C **15**, 2139 (1982).

[47] S. Bouarab, A. Vega, M. Lopez, M. P. Iniguez and J. A. Jensen, Phys. Rev. B **55**, 13279 (1997).

[48] S. L. Altmann and P. Hertzig, *Point-Group Theory Tables* (Clarendon Press, Oxford, 1994).